RESEARCH PAPER

Anti-Breast Cancer Potential of Biosynthesized Iron Oxide Nanoparticles Using Oxalis corniculata

Mr. Lalatendu Mohanty[1], Tusar Mishra[2*], Dr. Vijay Jyoti Kumar[3], Dr. Bhawana Sati[4], Dr. Hemlata Bhatt[5], Dr. Debasish Pradhan[6], Nitish Kumar[7]

[1]Assistant Professor, Department of Pharmaceutical Science, HNB Garhwal University, Uttarakhand, India.
Email: lituindia1@gmail.com (ORCID: 0009-0006-0177-6590)
[2*]Assistant Professor, Department of Pharmaceutical Science, Gaytri College of Pharmacy, Odisha, India.
Email: tusarmishra741@gmail.com (ORCID: 0009-0009-0838-1200) (***Corresponding Author**)
[3]Associate Professor, Department of Pharmaceutical Science, HNB Garhwal University, Uttarakhand, India.
Email: vjhnbgu@gmail.com
[4]Assistant Professor, Department of Pharmacy, Banasthali Vidyapith, Rajasthan, 304022, India.
Email: bhawanasati28@gmail.com
[5]Assistant Professor, Department of Pharmaceutical Science, HNB Garhwal University, Uttarakhand, India.
Email: visithemlata@yahoo.co.in
[6]Department of Pharmaceutical Sciences, Utkal University, Bhubaneswar, Odisha, India.
Email: drdebasishpradhan@utkaluniversity.ac.in
[7]Master of Pharmacy, Department of Pharmaceutical Science, HNB Garhwal University, Uttarakhand, India.

ABSTRACT

This study investigates the anticancer potential of iron oxide nanoparticles synthesized through a green method using Oxalis corniculata leaf extract. The formation of nanoparticles was initially confirmed by a visible colour change from yellow to brown, followed by validation using UV–Visible spectroscopy. Phytochemical analysis indicated the presence of flavonoids, which likely act as reducing and capping agents during synthesis. Scanning Electron Microscopy (SEM) revealed nanoparticles with a smooth surface and a thin coating layer, attributed to flavonoid capping. Transmission Electron Microscopy (TEM) confirmed that the nanoparticles are spherical and within the nanoscale size range. Zeta potential analysis suggested good stability of the nanoparticles, while Dynamic Light Scattering (DLS) indicated a polydisperse nature, which was identified as a limitation of the study. The anticancer activity was evaluated using the MCF-7 breast cancer cell line, where the nanoparticles demonstrated significant cytotoxic effects. Increased concentrations of the nanoparticles led to higher cancer cell death and reduced cell density. Overall, the study highlights the promising role of green-synthesized iron oxide nanoparticles as an alternative anticancer strategy, combining nanotechnology with the therapeutic benefits of plant-derived bioactive compounds, and provides a foundation for future clinical research.

Keywords: Iron oxide nanoparticles, MTT assay, SEM, TEM, DLS, Flavonoids.

How to cite this article: Mohanty L, Mishra T, Kumar VJ, Sati B, Bhatt H, Pradhan D, Kumar N. Anti-Breast Cancer Potential of Biosynthesized Iron Oxide Nanoparticles Using Oxalis corniculata. Int J Drug Deliv Technol. 2026;16(56s): 980-990. DOI: 10.25258/ijddt.16.56s.104

Source of support: Nil.
Conflict of interest: None.

1.Introduction- Cancer is a major global health challenge, with 19.3 million new cases and around 10 million deaths reported in 2020, projected to reach 30.2 million cases by 2040. It is characterized by uncontrolled cell growth influenced by genetic, environmental, and infectious factors, with lung cancer causing the highest mortality. Low- and middle-income countries account for nearly 70% of deaths due to limited healthcare access. Although treatments like chemotherapy, radiotherapy, and surgery are widely used, they face limitations such as side effects, drug resistance, and treatment interruptions. Conventional nanoparticle synthesis methods, including physical and

chemical approaches, also raise concerns due to toxicity, high energy use, and environmental hazards.[1]

Nanoparticle synthesis methods are mainly divided into physical and chemical approaches. Physical techniques such as laser ablation, mechanical milling, and vapor deposition, and chemical methods including co-precipitation, thermal decomposition, sol–gel, and chemical reduction are widely used. However, for biomedical nanoparticles like iron oxide nanoparticles, these methods often face limitations in achieving precise control over size, shape, and surface properties required for safe and effective applications [2].

Synthesis of nanostructured materials follows two basic approaches: (a) "Top-down" approach involves breaking down the bulk material into nanometre-sized grains or particles, and (b) "Bottom-up" approach involves building individual atoms/molecules to form the required nanoparticles. [3]. In the "top-down" approach, it involves various methods such as milling, photo lithography, electron beam lithography, ion- and plasma etching (PE), and anodization, etc., whereas in the "bottom-up" approach, which involves sol-gel, electrodepositions, laser pyrolysis, plasma or flame spraying synthesis, chemical vapor deposition (CVD), and bio-assisted synthesis.[4]. Importance of wound healing- Wound healing is a vital biological process that restores tissue integrity and function after injury. It plays an essential role in maintaining overall health and preventing complications that could result from tissue damage. The importance of wound healing can be understood through various perspectives.[5]

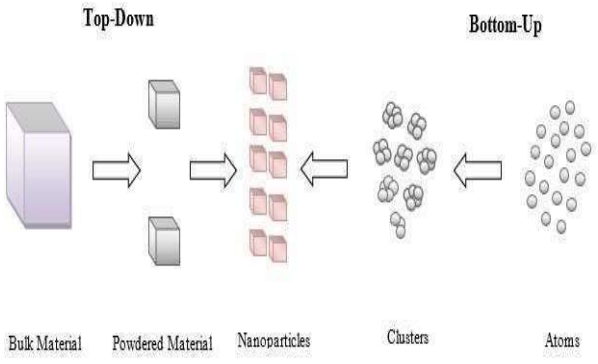

Chemical synthesis of metal nanoparticles enables rapid, large-scale production but often faces stability issues in aqueous media, leading to aggregation without stabilizing agents. Common capping agents like polyvinylpyrrolidone and sodium polyacrylate may cause particle deformation, reduced activity, and toxic by-product formation. Nanomaterials are broadly classified into organic-based (e.g., fullerenes, nanotubes) and inorganic-based (e.g., metal oxides, metals, quantum dots).[6] Physical synthesis methods, such as UV irradiation and microwave-assisted techniques, produce well-defined nanoparticles but are costly and time-consuming. Bimetallic nanoparticles exhibit structures like core–shell, alloy, and cluster-in-cluster, and are widely used in MRI imaging and magnetic hyperthermia for cancer treatment.[7]

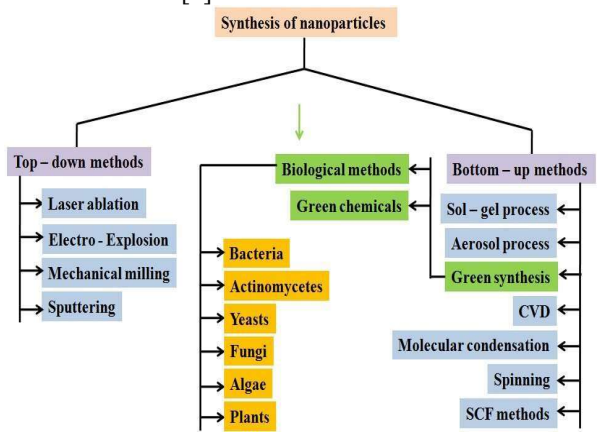

The size of iron oxide nanoparticles plays a vital role in determining their magnetic properties and suitability for biomedical applications. In most medical uses, these nanoparticles typically measure between 10 and 20 nm in diameter. For example, a nanoparticle with a 10 nm iron oxide core is often considered ideal, as it provides an optimal balance between superparamagnetic characteristics and biocompatibility.[8]

Green synthesis uses eco-friendly biological or natural materials to produce nanoparticles while reducing toxic chemicals and energy consumption. This method is especially important for synthesizing biocompatible nanoparticles, such as iron oxide nanoparticles, for biomedical applications including drug delivery and cancer therapy. [9] Plant-mediated synthesis employs plant extracts as reducing and stabilizing agents, where bioactive compounds convert metal ions into nanoparticles and prevent aggregation,

offering a simple and widely accessible synthesis approach.[9]

Green synthesis employs eco-friendly biological sources, particularly plant extracts rich in flavonoids, to produce iron oxide nanoparticles (IONPs) with reduced toxicity and improved stability. Superparamagnetic IONPs (SPIONs) are widely used in cancer therapy due to their unique magnetic properties, enabling targeted drug delivery and minimizing off-target effects. They overcome limitations such as poor drug solubility, rapid clearance, and multidrug resistance. IONPs can generate localized heat under an alternating magnetic field, inducing cancer cell death while sparing healthy tissues.[10] Additionally, they act as carriers for drugs and genetic materials, ensuring protection, controlled release, and enhanced therapeutic efficiency in cancer treatment.[11][12]

2.Plant Profile- *Oxalis corniculata,* commonly known as "Creeping woodsorrel", Indian sorrel, or Changeri in Ayurveda, is a small, herbaceous plant belonging to the Oxalidaceae family.
Terpenoids, alkaloids, flavonoids, glycosides, phenols, and other secondary components. Bioactive chemicals found in medicinal plants may have anti-cancer effects and attack cancer in a variety of ways. Nevertheless, they are still issues with clinical validation and standardisation, which calls for multidisciplinary research to fully realise their promise in cancer therapy. While there is still debate about the exact

native range of Oxalis corniculata, it is generally believed to be native to southeastern Asia or parts of the Mediterranean basin. Some botanical scholars also propose its origin in Europe, particularly the southern and western parts. Terpenoids, alkaloids, flavonoids, glycosides, phenols, and other secondary components. Bioactive chemicals found in medicinal plants may have anti-cancer effects and attack cancer in a variety of ways. Nevertheless, they are still issues with clinical validation and standardisation, which calls for multidisciplinary research to fully realise their promise in cancer therapy. Because they are strong anti-cancer agents and modulate tumour aggressiveness, phytochemicals are an excellent treatment for anaplastic thyroid, breast, and other malignancies.

3.Methods- **Preparation of Plant Leaf Extract:** Fresh *Oxalis corniculata* leaves were collected from a clean, pesticide-free area, thoroughly washed, and shade-dried in a ventilated space for 5–6 days with regular turning to avoid fungal growth.
The plant was authenticated by a taxonomist or botanical expert to ensure correct identification.[13]

Preparation of leaf powder: Fresh or dried, high-quality leaves were accurately weighed using a calibrated balance to ensure optimal extraction yield. The leaves were then ground into a fine powder using a mortar, pestle, or grinder to increase surface area for efficient extraction of water-soluble compounds.[14]

Extraction of leaf: The powdered leaves were mixed with distilled water in a 1:10 (w/v) ratio, stirred, and soaked for 1–2 hours at room temperature to extract bioactive compounds. For improved extraction, the mixture was heated at 50–60 °C for 60–90 minutes with continuous stirring, avoiding boiling to protect heat-sensitive compounds.[15]

Filtration of extract solution: The extract was filtered repeatedly using Whatman No. 1 filter paper to obtain a clear solution free of debris.
It was stored in amber containers at 4°C, and its pH (4.0–6.0) was measured to ensure stability of bioactive compounds.[16]

Preparation of Oxalis corniculata leaves extract.

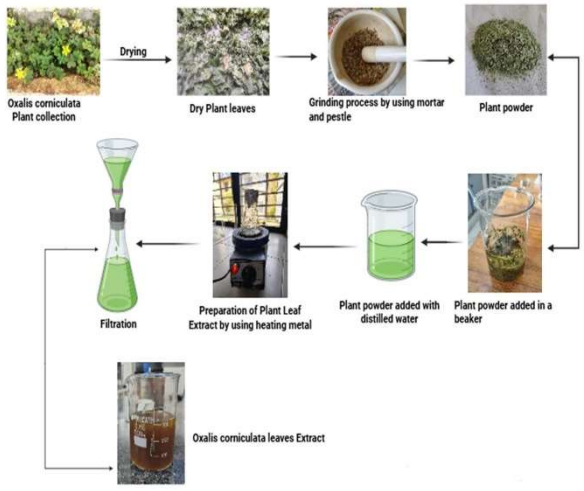

Preparation of Ferric Chloride Hexahydrate ($FeCl_3 \cdot 6H_2O$) Solution: Ferric chloride hexahydrate ($FeCl_3 \cdot 6H_2O$) is a hygroscopic yellowish-brown crystalline solid that must be handled quickly to avoid moisture absorption. Accurately 2.7029 g was weighed using a calibrated balance and transferred to a clean, dry 500 mL beaker. About 500 mL of distilled water was added to dissolve the compound completely. The solution was stirred using a glass rod or magnetic stirrer until a clear yellowish-brown solution formed.

The pH was measured (typically 1.5–2.5), indicating acidic nature due to hydrolysis.[17]

Preparation of Iron Oxide Nanoparticles by Green Synthesis Process: Green synthesis is a sustainable approach to nanoparticle production that utilizes natural,

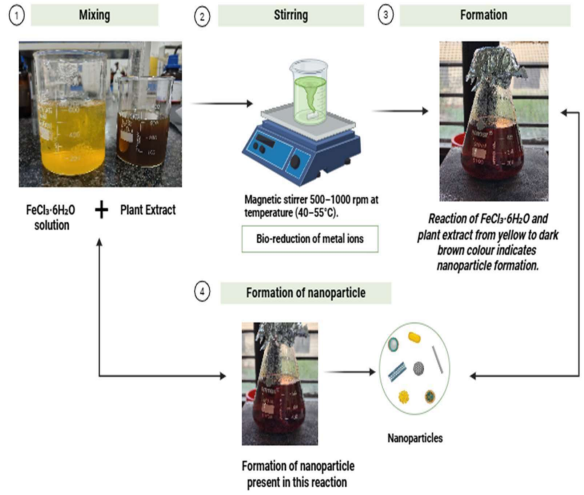

biodegradable, and non-toxic materials to reduce metal salts like iron (III) chloride hexahydrate ($FeCl_3 \cdot 6H_2O$) into nanoparticles.[18]

$FeCl_3 \cdot 6H_2O$, is a yellowish-brown crystalline compound, it is water-soluble, reactive precursor widely used for synthesizing iron-based nanoparticles. The plant extract was added dropwise to the $FeCl_3$ solution under continuous magnetic stirring. The ratio of extract to solution was adjusted based on reducing strength and desired nanoparticle size.[19]

The reaction mixture was stirred at room temperature and then heated to 40–55°C with continuous stirring (500–1000 rpm) to enhance reduction while preventing aggregation.

The process continued for 30 minutes to 3 hours until a colour change from yellow to dark brown indicated nanoparticle formation.

The pH was adjusted from 2.5–3.2 to around 8–8.5 using 0.1 N NaOH to facilitate synthesis.

Finally, the mixture was left at room temperature for 24 hours to complete the reduction process.[20]

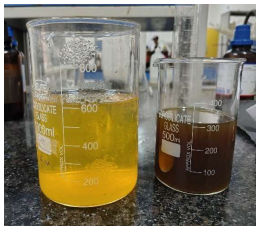

Reaction mixture of $FeCl_3 \cdot 6H_2O$ and plant extract.

The reaction mixture was transferred to a centrifuge tube, and the mixture was centrifuged at 4000 rpm for 7 minutes to separate nanoparticles from the supernatant: The nanoparticles were dried and washed using a vacuum oven at 50–60°C to prevent oxidation. The dried nanoparticles were stored in an airtight, dark container at room temperature to prevent moisture absorption and degradation.[21]

Process of Green Synthesis of Iron Oxide Nanoparticles.

Formation of Nanoparticles under the ratio of 2:3.

Characterization of Iron Oxide Nanoparticles: Surface plasmon resonance (SPR) and the absorption peaks were determined, found to be at a wavelength of 360nm, indicating the formation of nanoparticles. Reference value

for the formation of a nanoparticle is (290–370) nm. Surface morphology and agglomeration of nanoparticles were examined using SEM, providing details on size, shape, surface texture, and aggregation.[22] SEM revealed

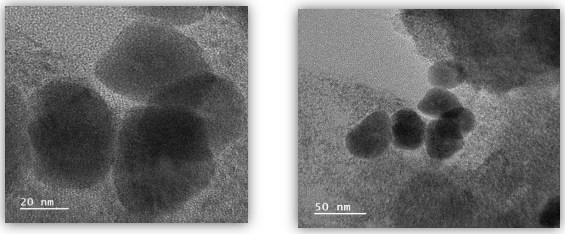

biomolecule coatings and particle shapes (spherical, cubic, or irregular), typically ranging from 10–100 nm.[23] TEM provides high-resolution visualization of nanoparticle size (typically 5– 50 nm), shape, and distribution, revealing morphology influenced by synthesis conditions and biomolecule coatings. It helps identify particle shapes, aggregation behaviour, and surface organic layers affecting stability and performance.[24] Zeta potential reflects the surface charge and colloidal stability of green-synthesized iron oxide nanoparticles. These nanoparticles typically show negative zeta potentials (−20 to −40 mV) due to anionic biomolecules from plant extracts. Surface functional groups adsorbed during the reduction of $FeCl_3 \cdot 6H_2O$ play a key role in enhancing nanoparticle stability.[25] DLS measures nanoparticle size based on their Brownian motion in a liquid medium. Laser light scattering and intensity fluctuations are analyzed to determine particle size distribution.[25]

A stock solution was prepared using the sample in 0.1% HCl and DMSO, then diluted with DMEM to obtain working concentrations.

MCF-7 cells were seeded in 96-well plates and incubated until 70–80% confluence.

Cells were treated with different concentrations of the sample for 24 hours, and morphological changes were observed. Cytotoxicity was evaluated using the MTT assay by measuring absorbance at 570 nm after dissolving formazan crystals to determine cell viability.[26]

Cell viability (%) — (Absorbance of sample/Absorbance of control) X 100[16]

4. Result-

1. Confirmation of iron oxide nanoparticle formation by UV-Vis Spectroscopy: UV–vis spectroscopy is commonly used to confirm nanoparticle synthesis by detecting surface plasmon resonance from collective electron oscillations. Iron oxide nanoparticles show SPR absorption typically between 290–370 nm. This rapid, non-destructive method allows real-time monitoring of synthesis progress. This technique is rapid and non-destructive, suitable for monitoring the reaction progress in real-time. (Mittal et al., 2013; Singh et al., 2018). Our sample shows Surface plasmon resonance (SPR) and absorption peaks at 360nm, indicating the formation of nanoparticles. This clearly indicates the formation of Iron oxide nanoparticles. Resulting from the successful reduction by phytochemicals present in Oxalis corniculata extract.

UV-Visible spectrum of iron oxide nanoparticles

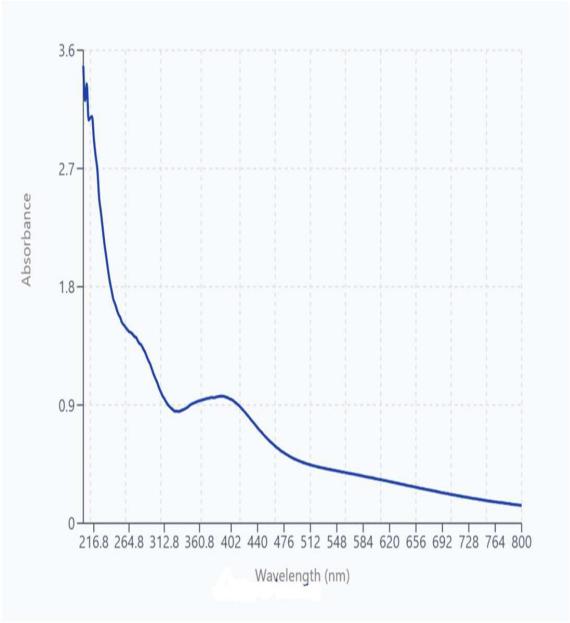

showing an absorption peak at 360 nm.

Phytochemicals such as flavonoids and terpenoids act as reducing and stabilizing agents, preventing nanoparticle agglomeration. The appearance of the SPR band, absent in the plant extract and $FeCl_3 \cdot 6H_2O$, confirms nanoparticle formation.

2.**SEM (scanning electron microscopy) Analysis:** The average particle size is expected to be in the range of 10–100 nm, as observed in similar green synthesis studies. SEM images typically show a smooth surface with a thin organic layer, attributed to the capping action of phytochemicals like flavonoids and phenolic compounds.

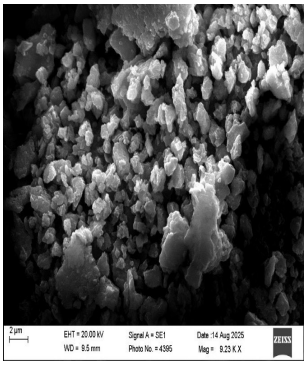

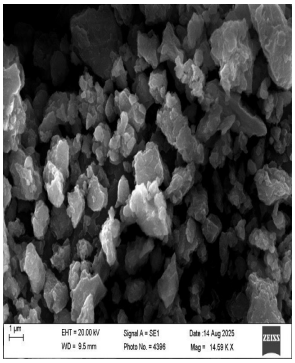

The organic coating enhances nanoparticle stability but may obscure some surface details in SEM images. Moderate aggregation occurs, though plant-derived stabilizers improve dispersion and confirm phytoconstituent adsorption on the surface.

3.**TEM (transmission electron microscope) Analysis:** Transmission Electron Microscopy (TEM) was utilized to better understand the morphology features and size particles (NPs). TEM ticle morphology and 100 nm). IONPs: ~20–

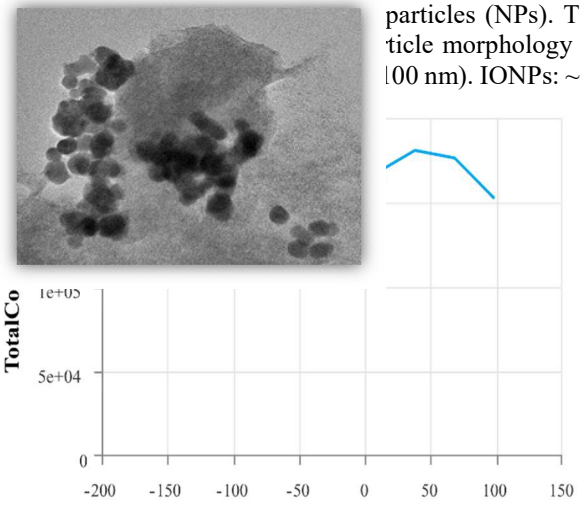

50 nm, spherical, uniform size. Micrographs sized 20nm to 50nm are shown in the figures. the size of nanoparticles in the range from 20 to 50nm, approximately spherical shape, and uniformity. The nanoparticles exhibit a uniform size and show minimal aggregation. The TEM image displays synthesized Nanoparticles in a size range of 20nm to 50nm at different magnifications, showcasing distinct spherical nanoparticles, exhibiting a uniform size, and demonstrating minimal aggregation. The TEM figure displays synthesized Nanoparticles at a lower magnification and shows the overall distribution of distinct spherical nanoparticles, exhibiting a uniform size and demonstrating minimal aggregation.**4. Zeta Potential Analysis:** Zeta potential is a measure of the electrical charge at the surface of nanoparticles in a colloidal suspension, specifically at the slipping plane of the electrical double layer surrounding the particle. It is expressed in millivolts (mV).

Zeta Potential (mv)

Phase Plot:

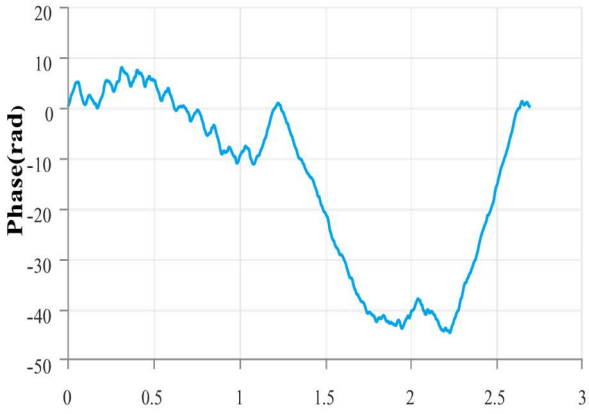

	Name	Mean	Standard Deviation	RSD	Minimum	Maximum
1	Zeta Potential (mV)	-96	-	-	-96	-96
2	Zeta Peak 1 Mean (mV)	-82.11	-	-	-82.11	-82.11
3	Zeta Peak 2 Mean (mV)	38.37	-	-	38.37	38.37
4	Conductivity (mS/cm)	0.2135	-	-	0.2135	0.2135
5	Wall Zeta Potential (mV)	0	-	-	0	0
6	Zeta Deviat	1075	-	-	1075	10

	ion (mV)					75
7	Derived Mean Count Rate (kcps)	313	-	-	313	313
8	Reference Beam Count Rate (kcps)	1316	-	-	1316	13116
9	Quality Factor	0.9005	-	-	0.9005	0.90005

Biomolecules such as polyphenols, proteins, and flavonoids from plant extracts coat IONPs, providing functional groups that enhance surface charge and stability. These groups increase the absolute zeta potential, improving nanoparticle dispersion and preventing aggregation. Graph analysis shows charge variation, with one trend peaking between 50–100 and another fluctuating between −50 to 10 mV. The zeta potential distribution is unimodal, with a dominant peak at −96 mV. This high negative value (> ±30 mV) indicates excellent colloidal stability and successful nanoparticle formation.

5.DLS: Dynamic Light Scattering: Dynamic Light Scattering (DLS), also known as photon correlation spectroscopy or quasi-elastic light scattering, is a widely used analytical technique for characterizing nanoparticles (NPs) in suspension, particularly in the context of green synthesis.

Size (dnm)

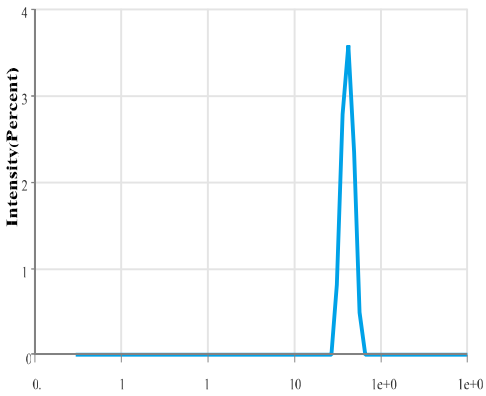

DLS is used to measure the hydrodynamic diameter and polydispersity index (PDI) of nanoparticles in suspension. The hydrodynamic diameter includes both the particle and its surface-bound molecules, reflecting overall size in solution. PDI indicates the uniformity of particle size distribution, with ideal monodisperse systems having PDI <0.2. In this study, the PDI value is 0.7956, indicating a highly polydisperse system. Such nanoparticles are less uniform but may still be suitable for applications where strict size uniformity is not required.

6.Phytochemical constituent test of Oxalis corniculata:

Statistics Table						
Name		Mean	Standard Deviation	RSD	Minimum	Maximum
1	Z-Average (nm)	457.2	-	-	457.2	457.2
2	Polydispersity Index (PI)	0.7956	-	-	0.7956	0.7956
3	Intercept	0.9131	-	-	0.9131	0.9131
4	Peak 1 Mean by Intensity ordered by area (nm)	418.3	-	-	418.3	418.3
5	Peak 1 Area by Intensity ordered by area (%)	100	-	-	100	100
6	Derived Mean Count Rate (kcps)	1407	-	-	1407	1407

Phytoconstituent	Test Performed	Observation	Result (+/-)
Terpenoids	Salkowski Test	Yellow color at the interface of the two layers.	+

		yellow color.	

Concentrations (µg /mL)	Absorbance			Average	Cell Viability	Inhibition %
	1	11				
Control	0.805	0.812	0.819	0.812	100.000	0.000
12.5	0.788	0.796	0.784	0.789	97.209	2.791
25	0.687	0.675	0.667	0.676	83.292	16.708
50	0.399	0.41	0.394	0.401	49.384	50.616
100	0.189	0.193	0.18	0.187	23.071	76.929
200	0.095	0.101	0.09	0.095	11.741	88.259

	Sulfur Powder Test	No clear observation was mentioned.	± (Inconclusive)
Flavonoids	Lead Acetate Test	Yellow precipitate formed.	+
	KOH Test	The yellow color appeared.	+
	Alkaline Reagent Test	Yellow to pale color.	+
	Zinc-HCl Test	Red, orange, or yellow color.	+
	H2SO4 Test	Deep yellow color.	+
	Shinoda Test	Red, orange, or	+

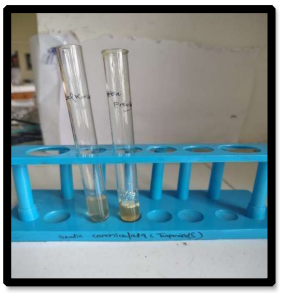

7.Anticancer Evaluation of Iron Oxide Nanoparticles: Green synthesis methods using plant extracts such as Oxalis corniculata have further enhanced the biocompatibility and functionalization potential of IONPs

Drug response curve of iron oxide

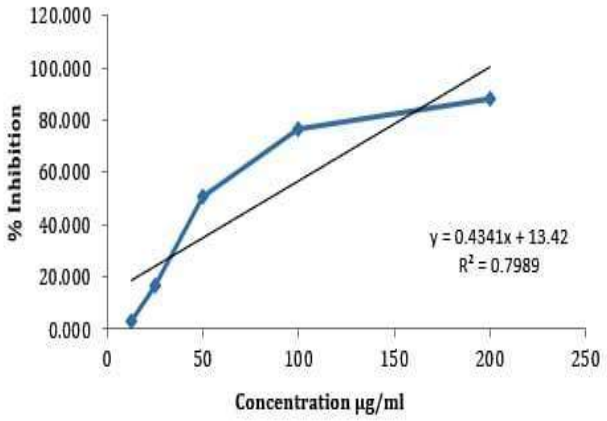

nanoparticles (concentration vs percentage of inhibition of the cancer cell). A higher R^2 suggests that your model's predictions closely match the actual data. Value of R^2 = 0.7889(approx 0.80) indicates that 80 %of the variation in the dependent variable can be explained by the independent variable in the model. The remaining 20% of variation is not explained by the model and may be due to other factors/random error.

(R^2 ranges from 0 to 1, and it indicates how the regression line fits the data)

Cytotoxicity assay of Iron oxide nanoparticles showing anticancer effect on MCF-7 cell line under 100µm range

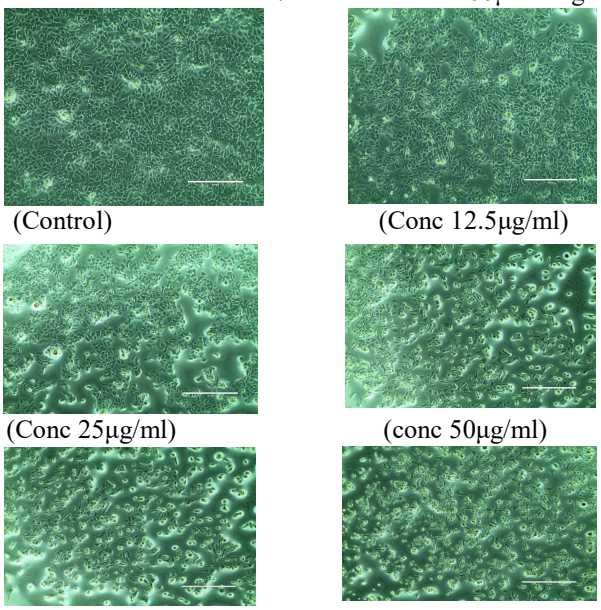

(Control) (Conc 12.5µg/ml)

(Conc 25µg/ml) (conc 50µg/ml)

(Conc 100µg/ml) (Conc 200µg/ml)

Interpretation: The IC50 value of Iron oxide nanoparticles against MCF-7 Cells was found to be 84.266 µg /ml. Morphological observation of cells shows that increasing cytotoxicity and decreasing cell density of MCF-7 cells occur with an increase in test concentration treatment. The synergistic combination of iron oxide nanoparticles and flavonoids from Oxalis corniculata offers strong potential for green cancer nano therapy. Plant flavonoids act as reducing and capping agents, enhancing stability, biocompatibility, and targeting of iron oxide nanoparticles (IONPs). Quercetin-loaded IONPs improve anticancer efficacy by increasing cellular uptake, enabling controlled release, and boosting ROS-mediated apoptosis in MCF-7-cells. IONPs facilitate tumour targeting via the EPR effect and amplify oxidative stress through Fenton-like reactions, enhancing caspase activation. The synergy induces apoptosis and ferroptosis in cancer cells while flavonoids protect normal cells through selective antioxidant action.

Conclusion: In this study, iron oxide nanoparticles (IONPs) were successfully synthesized using an eco-friendly, cost-effective green method employing *Oxalis corniculata* leaf extract as both reducing and capping agent. The flavonoid-rich extract enabled simultaneous nanoparticle formation and therapeutic flavonoid loading, offering synergistic anticancer effects. UV–Vis analysis confirmed nanoparticle formation with an SPR peak around 360 nm. SEM and TEM revealed predominantly spherical nanoparticles with sizes ranging from 20–50 nm and an organic phytochemical coating that enhanced stability. Zeta potential analysis (−96 mV) indicated excellent colloidal stability, while DLS showed moderate polydispersity. Phytochemical tests confirmed flavonoid presence on nanoparticles. Anticancer evaluation using the MCF-7 cell line demonstrated significant cytotoxicity with an IC_{50} of 84.266 µg/mL and dose-dependent cell inhibition. Overall, green-synthesized, flavonoid-loaded IONPs show strong potential for sustainable cancer nano therapy, warranting further investigation.

REFERENCES:

1. Siegel, R. L., Miller, K. D., Fuchs, H. E., & Jemal, A. (2020). Cancer statistics, 2020. *CA: A Cancer Journal for Clinicians*, 70(1), 7–30. https://doi.org/10.3322/caac.21590
2. Blanco Carcache, P. J., Addo, E. M., & Kinghorn, A. D. (2021). Higher plant sources of cancer chemotherapeutic agents and the potential role of biotechnological approaches for their supply. In H. M. Ekiert, K. G. Ramawat, & J. Arora (Eds.), *Medicinal plants: Domestication, biotechnology and regional importance* (pp. 1–28). Springer.
3. Balapure, K., Jain, R., & Bhargava, S. (2015). Green synthesis of silver nanoparticles using neem extract and their application in dye degradation. *Journal of Hazardous Materials*, 297, 147–154. https://doi.org/10.1016/j.jhazmat.2015.04.074
4. Mody, V. V., Siwale, R., Singh, A., & Mody, H. R. (2010). Introduction to metallic nanoparticles. *Journal of Pharmacy and Bioallied Sciences, 2*(4), 282–289. https://doi.org/10.4103/0975-7406.72127
5. Chawra, H. S., Kumar, V., & Patel, R. (2023). Nanoparticles for cancer therapy: Current progress and challenges. *Discover Nano*, 18(1), 150. Bayat Mokhtari, R., Homayouni, T. S., Baluch, N., Morgatskaya, E., Kumar, S., Das, B., & Yeger, H. (2017). Combination therapy in combating cancer. *Oncotarget*, 8(23), 38022–38043.
6. Dubey, S. P., Lahtinen, M., & Sillanpää, M. (2010). Green synthesis and characterizations of silver and gold nanoparticles using leaf extract of Rosa rugosa. *Colloids and Surfaces A: Physicochemical and Engineering Aspects, 364*(1–3), 34–41. https://doi.org/10.1016/j.colsurfa.2010.04.023
7. Chandran, S. P., Chaudhary, M., Pasricha, R., Ahmad, A., & Sastry, M. (2006). Synthesis of gold nanotriangles and silver nanoparticles using Aloe vera plant extract. *Biotechnology Progress, 22*(2), 577–583. https://doi.org/10.1021/bp0501423

8. Akinmoladun, F. O., Akinrinlola, B. L., Komolafe, T. O., Farombi, E. O., & Olaleye, T. M. (2020). Green synthesis of nanoparticles using medicinal plants and their biomedical applications. *Nanotechnology Reviews, 9*(1), 185–200. https://doi.org/10.1515/ntrev-2020-0015
9. Kulkarni, A. D., & Muddapur, U. M. (2014). Biosynthesis of metal nanoparticles: A review. *Journal of Nanotechnology*, 2014, 1–8. https://doi.org/10.1155/2014/510246
10. Mohan, A., Garg, A., Gupta, A., Sahu, S., Choudhari, C., Vashistha, V., Ansari, A., Pandey, R., Bhalla, A. S., & Madan, K. (2020). Clinical profile of lung cancer in North India: A 10-year analysis of 1862 patients from a tertiary care center. *Lung India*, 37(3), 190–197. https://doi.org/10.4103/lungindia.lungindia_333_19
11. Wang, M., & Thanou, M. (2010). Targeting nanoparticles to cancer. *Pharmacological Research*, 62(2), 90–99. https://doi.org/10.1016/j.phrs.2010.03.005
12. Meyers, M. A., Mishra, A., & Benson, D. J. (2006). Mechanical properties of nanocrystalline materials. *Progress in Materials Science*, 51(4), 427–556. https://doi.org/10.1016/j.pmatsci.2005.08.003
13. Ali, S., & Shahid, M. (2021). Green synthesis of iron oxide nanoparticles using plant extracts: A review. *Journal of Molecular Structure*, 1242, 130759.
14. Devi, L. S., & Joshi, S. R. (2012). Antimicrobial and antioxidant properties of different solvent extracts of *Oxalis corniculata* Linn. *International Journal of Pharma and Bio Sciences*, 3(2), 622–628.
15. Sathishkumar, M., et al. (2010). Green synthesis of silver nanoparticles using *Musa sapientum* (banana) leaf extract and its antibacterial activity. *Spectrochimica Acta Part A: Molecular and Biomolecular Spectroscopy*, 82(3), 1035–1041.
16. Blanco Carcache, P. J., Addo, E. M., & Kinghorn, A. D. (2021). Higher plant sources of cancer chemotherapeutic agents and the potential role of biotechnological approaches for their supply. In H. M. Ekiert, K. G. Ramawat, & J. Arora (Eds.), *Medicinal plants: Domestication, biotechnology and regional importance* (pp. 1–28). Springer.
17. Parveen, K., Banse, V., & Ledwani, L. (2016). Green synthesis of nanoparticles: Their advantages and disadvantages. *AIP Conference Proceedings*, 1724(1), 020048. https://doi.org/10.1063/1.4945168
18. Ahmed, S., Ahmad, M., Swami, B. L., & Ikram, S. (2016). Green synthesis of silver nanoparticles using Azadirachta indica aqueous leaf extract. Journal of Advanced Research, 7(1), 17-28.
19. Singh, J., Dutta, T., Kim, K.-H., Rawat, M., Samddar, P., & Kumar, P. (2018). 'Green' synthesis of metals and their oxide nanoparticles: Applications for environmental remediation. Journal of Nanobiotechnology, 16, 84.
20. Kgosiemang, I. K. R., Adegoke, A. M., Mashele, S. S., & Sekhoacha, M. P. (2023). Green synthesis of iron oxide and iron dioxide nanoparticles using *Euphorbia tirucalli*: Characterization and antiproliferative evaluation against three breast cancer cell lines. *Journal of Experimental Nanoscience, 18*(1), 2276276. https://doi.org/10.1080/17458080.2023.2276276
21. Aida, M. S., Alonizan, N., Zarrad, B., & Hjiri, M. (2023). Green synthesis of iron oxide nanoparticles using Hibiscus plant extract. *Journal of Taibah University for Science, 17*(1), 2221827. https://doi.org/10.1080/16583655.2023.2221827
22. Ahmed, I., Mir, F. A., & Banday, J. A. (2023). Synthesis of metal and metal oxide nanoparticles using plant extracts—Characterization and applications. *BioNanoScience, 13*(5), 1541–1557. https://doi.org/10.1007/s12668-023-01194-y
23. Kokate, C. K., Purohit, A. P., & Gokhale, S. B. (2021). Pharmacognosy. Nirali Prakashan.
24. T. Mossmann, Rapid colorimetric assay for cellular growth and survival: application to proliferation and cytotoxicity assays, J. Immunol. Methods 65 (1983) 55—63.
25. Sirelkhatim, A., Mahmud, S., Seeni, A., Kaus, N. H. M., Ann, L. C., Bakhori, S. K. M., Hasan, H., & Mohamad, D. (2015). Review on zinc oxide nanoparticles: Antibacterial activity and toxicity mechanism. Nano-Micro Letters, 7(3), 219–242. https://doi.org/10.1007/s40820-015-0040-x
26. Kumar, A., & Mandal, D. (2017). Synthesis and applications of metal oxide nanoparticles: A review. *Materials Today: Proceedings*, 4(4), 5464–5470. https://doi.org/10.1016/j.matpr.2017.05.007